FULL PAPER

Dalton
www.rsc.org/dalton

# Synthesis, structure and properties of [Pt(2,2′-bipyridyl-5,5′-dicarboxylic acid)(3,4-toluenedithiolate)]: tuning molecular properties for application in dye-sensitised solar cells

**Elaine A. M. Geary,[a] Narukuni Hirata,[b] John Clifford,[b] James R. Durrant,[b] Simon Parsons,[a] Alice Dawson,[a] Lesley J. Yellowlees[a] and Neil Robertson *[a]**

[a] *School of Chemistry, Joseph Black Building, Kings Buildings, West Mains Road, Edinburgh, UK EH9 3JJ. E-mail: neil.robertson@ed.ac.uk; Fax: +441316504743; Tel: +441316504755*

[b] *Centre for Electronic Materials and Devices, Department of Chemistry, Imperial College, London, UK SW7 2AZ*

***Received 3rd June 2003, Accepted 15th August 2003***
***First published as an Advance Article on the web 27th August 2003***

The platinum diimine dithiolate complex, [Pt(2,2′-bipyridyl-5,5′-dicarboxylicacid)(3,4-toluenedithiolate)] ([Pt(5,5′-dcbpy)(tdt)]) and its tetrabutylammonium salt $[TBA]_2$[Pt(5,5′-dcbpy)(tdt)] have been prepared, spectroscopically and electrochemically characterised and attached on to $TiO_2$ substrate to be used as solar cell sensitisers. A single-crystal X-ray structure was obtained for $[TBA]_2$[Pt(5,5′-dcbpy)(tdt)]·EtOH·EtOAc. The effect of the position of the two carboxylic acid substituents on the electrochemistry of the 5,5′-disubstituted complexes is discussed in comparison with the previously reported [Pt(4,4′-dcbpy)(tdt)]. Electrochemical studies show no major change in the HOMO after movement of the carboxylic acid groups, consistent with assignment of the HOMO as largely dithiolate based. Movement of the carboxylic acid groups makes the diimine electronic character and hence the LUMO of the complexes different. Electrochemical studies show a change to lower energy of the LUMO represented by changes in reduction potential of the compound on moving the carboxylic acid substituents from the 4,4′ to the 5,5′ positions. Both [Pt(5,5′-dcbpy)(tdt)] and $[TBA]_2$[Pt(5,5′-dcbpy)(tdt)] have been used as solar cell sensitisers, with the di-TBA salt giving lower dye loading but superior photovoltaic performance. The consequences of tuning the complex through the position of the carboxylic acid groups are discussed.

## Introduction

Over the past decade the charge transfer excited state of a series of square-planar compounds of the general formula Pt(II)-(diimine)(dithiolate) has been investigated.[1–3] These complexes have shown room-temperature solution luminescence and a highly solvatochromic charge transfer (CT) absorption. Recent investigations have stated that the transition is a “Mixed Metal-Ligand-to-Ligand Charge-Transfer” (MMLL′CT) involving a HOMO which is a mixture of Pt(d) and dithiolate orbitals and a LUMO which is primarily a $\pi^*$ diimine orbital.[1,2] Subsituents on the diimine affect the electronic and photophysical properties of the LUMO while substituents on the dithiolate affect the HOMO properties. Tuning of these Pt(II)(diimine)(dithiolate) complexes, by ligand variation[3–8] has also shown that the excited state energies can be tuned by up to 1 eV.[1]

Tuning the electrochemical and photophysical properties of dyes is particularly relevant to the area of photovoltaic cells. In dye-sensitised solar cells, the dye molecule absorbs visible light and, after excitation injects electrons into the conduction band of a semiconductor ($TiO_2$). The oxidised dye molecule is subsequently reduced by electron donation from a redox system such as the iodide/triiodide couple. The function of these cells is crucially dependent on the optical and electrochemical properties of dyes.[1,2] The majority of dyes currently in use are short wavelength dyes and hence absorb at high energy. Longer wavelength dyes are desirable to allow absorption of light over a greater region of the solar spectrum and hence harvest more solar energy. All dyes previously investigated for solar cells contain some functional group present to attach the dye molecule to the $TiO_2$ surface. Most commonly 2,2′-bipyridyl-4,4′-dicarboxylic acid (4,4′-dcbpy) has been used, where the carboxylic acid groups anchor the dye molecule to $TiO_2$.[9]

In a study of bipyridinecarbonitirile complexes of Mo and W, however, Baxter and Connor concluded that the nitriles in the 5,5′ positions exert a greater electron withdrawing effect upon the metal than nitriles in the 4,4′ positions of the bpy ligand.[10] Furthermore, recent DFT calculations, electrochemical, spectroelectrochemical and EPR studies on [Pt(5,5′-$(X)_2$-bpy)$Cl_2$] complexes (X = H, Me, $CO_2Me$, $CO_2Et$, $NH_2$) showed that electron density at the 5,5′ positions is significantly greater than at the 4,4′ positions.[11,12] It is therefore expected that substituents at the 5,5′ positions would have a greater effect on the electronic character of the bpy than substituents at the 4,4′ positions.

5,5′-Disubstituted bipyridines have previously been investigated in Ru systems for use as sensitisers in solar cells.[13] Ru(5,5′-dcbpy)$_2$(X)$_2$, (where X = $Cl^-$, $CN^-$ and $SCN^-$) have been synthesised and used in solar cells and compared with the previously synthesised 4,4′-analogues. The (5,5′-dcbpy) compounds showed an enhanced spectral response at lower photon energies, however they were less efficient as solar cell sensitisers than the 4,4′ analogues. Pt(II)(diimine)(dithiolate) complexes have been recently investigated for their possible use as sensitisers in photovoltaic cells,[14,15] however studies were limited to complexes with 4,4′-dcbpy.

In this context we have studied [Pt(2,2′-bipyridyl-5,5′-dicarboxylicacid)(3,4-toluenedithiolate)] ([Pt(5,5′-dcbpy)(tdt)]) and its tetrabutylammonium salt ($[TBA]_2$[Pt(5,5′-dcbpy)(tdt)]). The related complex ([Pt(4,4′-dcbpy)(tdt)]) was previously investigated by Arakawa and co-workers.[15] By placing electron withdrawing groups at the 5,5′ positions of the bipyridyl group, we aim to lower the LUMO energy and investigate the effect on the optical and electrochemical properties and the performance in a dye-sensitised solar cell of a Pt-based dye molecule.

## Experimental

5,5′-Dimethyl-2,2′-bipyridine, 3,4-toluenedithiolate (tdt), purchased from Sigma-Aldrich and $K_2PtCl_4$ purchased from Johnson Matthey, were used as received.

DOI: 10.1039/b306241d

### Synthesis of 5,5′-dcbpy

5,5′-dcbpy was synthesised by a previously reported method.[16] Yield 95.1%. Found: C, 51.6; H, 3.1; N, 10.3. Calc. for $C_{12}H_8N_2O_4$: C, 52.0; H,3.3; N,11.5%. IR $\nu$/cm$^{-1}$: 1593s ($\nu_{asym}$CO), 1685s. $m/z$: 245 ($M^+$).

### Synthesis of [Pt(5,5′-dcbpy)Cl$_2$]

[Pt(5,5′-dcbpy)Cl$_2$] was synthesised by an analogous method to the 4,4′ analogue.[15] Yield 76.21%. Found: C, 28.8; H, 1.7; N, 5.5. $C_{12}H_8N_2O_4PtCl_2$ requires C, 28.3; H, 1.6; N, 5.5%. IR $\nu$/cm$^{-1}$: 1616s ($\nu_{asym}$CO). $m/z$: 510 ($M^+$).

### Synthesis of [Pt(5,5′-dcbpy)(tdt)]

[Pt(5,5′-dcbpy)Cl$_2$] (0.25 g, 0.49 mmol) was dissolved in a minimum amount of 0.1 M KOH (10 ml). To this mixture, tdt (0.11 g, 0.68 mmol) and 10 ml MeOH were added. A dark purple solution formed immediately and was allowed to stir for an additional 2 h. The product, [Pt(5,5′-dcbpy)(tdt)], was precipitated using 0.1 M HCl. The black precipitate was collected by filtration and washed with water. The crude product was redissolved in the minimum amount of 1 M KOH and purified by column chromatography using a Sephadex-LH 20 column, with water as the eluent. The main purple band was collected and precipitated as the neutral complex by addition of 0.1 M HCl. [Pt(5,5′-dcbpy)(tdt)] was isolated by filtration, washed with water and dried under vacuum. Yield 40.7%. Found: C, 36.1; H, 2.6; N, 4.2. $C_{19}H_{14}N_2O_4S_2Pt\cdot 2H_2O$ requires C, 36.2; H, 2.9; N, 4.5%. IR $\nu$/cm$^{-1}$: 1609m ($\nu_{asym}$CO). $m/z$ 593 ($M^+$).

### Synthesis of [TBA]$_2$[Pt(5,5′-dcbpy)(tdt)]

[Pt(5,5′-dcbpy)(tdt)] (0.05 g, 0.084 mmol) was dissolved in the minimum amount of 0.1 M KOH and 2 ml 0.1 M tetrabutylammoniumbromide (TBABr) was added. The product was extracted using dichloromethane (DCM). The DCM was evaporated and ether was added to the purple solid. Trituration of the solid and repeated washing with diethyl ether resulted in a magenta powder of [TBA]$_2$[Pt(5,5′-dcbpy)(tdt)]. Yield 50.5%. Calc. for $C_{51}H_{84}N_4O_4S_2Pt$: C, 56.9; H, 7.9; N, 5.2. Found: C, 56.6; H, 8.9; N, 4.6%. IR $\nu$/cm$^{-1}$: 1627s. $m/z$ 1077 ($M^+$).

### X-Ray crystallography

Crystal data for [TBA]$_2$[Pt(5,5′-dcbpy)(tdt)]·EtOH·EtOAc, $C_{57}H_{98}N_4O_7PtS_2$, $M$ = 1210.61. A purple block of dimensions 0.57 × 0.55 × 0.45 mm was used for data collection. The crystal structure was monoclinic, space group $P2_1/c$, $a$ = 16.4091(7), $b$ = 14.4709(6), $c$ = 27.5157(12) Å, $\beta$ = 105.5480(10)°, $V$ = 6294.6(5) Å$^3$ at $T$ = 150 K. $Z$ = 4, $D_c$ = 1.277 Mg m$^{-3}$, $\mu$ = 2.344 mm$^{-1}$. Diffraction data were collected with Mo-K$\alpha$ radiation on a Smart APEX CCD diffractometer equipped with an Oxford Cryosystems low-temperature device. An absorption correction was applied using the multi-scan procedure SADABS (range of transmission: 0.823–1.000).[17] The structure was solved by direct methods and refined by full-matrix least squares against $|F|^2$ using all data ($\theta_{max}$ = 28.95°) (SHEXTL);[18] hydrogen atoms were placed in idealised positions. The methyl group of the thiolate ligand was disordered over two positions; refinement of the relative weight of the components converged to 0.5 : 0.5, and this occupancy ratio was subsequently applied as a constraint. Difference electron density maps implied the presence of a disordered solvent region, and this (comprising 192 e per cell) was treated in the manner described by van der Sluis and Spek.[19] Calculation of the formula, $M$, $F$(000) *etc.* have assumed that this region corresponds to one molecule of ethyl acetate per formula unit. The refinement converged to $R1$ = 0.0301 [based on $|F|$ and 13231 data with $|F| > 4\sigma(|F|)$]; $wR2$ = 0.0802 (based on $|F|^2$ and all 15448 data) for 604 parameters. The final difference map extremes were +1.72 and −0.63 e Å$^{-3}$.

CCDC reference number 211901.

See http://www.rsc.org/suppdata/dt/b3/b306241d/ for crystallographic data in CIF or other electronic format.

### Other experimental

All UV-vis spectra were recorded on a Perkin-Elmer Lambda 9 spectrophotometer controlled by a Datalink PC, running UV/Winlab software.

Electrochemical studies were carried out using a DELL GX110 PC with General Purpose Electrochemical System (GPES), version 4.8, software connected to an autolab system containing a PGSTAT 20 potentiostat. The techniques used a three-electrode configuration, with a 0.5 mm diameter Pt disc working electrode, a Pt rod counter electrode and an Ag/AgCl (saturated KCl) reference electrode against which the ferrocenium/ferrocene couple was measured to be +0.55 V. The supporting electrolyte was 0.1 M tetrabutylammonium tetrafluoroborate (TBABF$_4$).

OTTLE (Optically Transparent Thin Layer Electrode) measurements were taken using a quartz cell of 0.5 mm, a Pt/Rh gauze working electrode, an Ag/AgCl reference electrode and a Pt wire counter electrode.[20] UV-vis spectra were recorded on a Perkin-Elmer Lambda 9 spectrophotometer, controlled by a Datalink PC, running UV/Winlab software. Spectroelectrochemical measurements were carried out on both [Pt(5,5′-dcbpy)(tdt)] and [TBA]$_2$[Pt(5,5′-dcbpy)(tdt)]. Ottle measurements on [Pt(5,5′-dcbpy)(tdt)] were carried out at 298 K in DMSO and at 233 K in a 1 : 3 solution of DMSO–MeCN. Ottle measurements on [TBA]$_2$[Pt(5,5′-dcbpy)(tdt)] were carried out at 233 K in DMF. 0.1 M TBABF$_4$ was used as the supporting electrolyte in all cases.

Electronic emission spectra were recorded on a Jobin Yvon Spex Fluoromax spectrofluorimeter, connected to a DSC Datalink PC running Instruments S.A. Datamax software. All emission spectra were recorded with [Pt(5,5′-dcbpy)(tdt)] dissolved in DMSO and dispersed in EtOH. All spectra were recorded in standard Wilmad 5 mm quartz NMR tubes contained in a liquid nitrogen filled fused silica Dewar.

Nanoporous TiO$_2$ thin films (8 μm thick) on conductive glasses were prepared as previously reported.[21] The size of the samples was 1 cm$^2$. The thin films were sensitised at room temperate for 22 h in 1.7 mM DMSO solution ([Pt(5,5′-dcbpy)(tdt)]) or 0.93 mM solution of ([TBA]$_2$[Pt(5,5′-dcbpy)(tdt)]) in 1 : 3.2 DMSO–MeCN. Transient absorption studies were carried out employing 610 nm excitation of the sensitiser dye, monitoring the photoinduced absorption of the TiO$_2$ electron at 1000 nm.[21] Photoelectrochemical measurements were performed as previously described employing ‘sandwich type’ photovoltaic cells with platinised counter electrode.[22] The electrolyte used contained 0.1 M LiI, 0.8 M TBAI, 0.1 M I$_2$, 0.5 M $^t$BuPy in acetonitrile. The working electrode had an illuminated surface area of 1.0 cm$^2$. Experiments were conducted under AM 1.5 simulated sunlight.

## Results and discussion

[Pt(5,5′-dcbpy)(tdt)] was synthesised by a route analogous to [Pt(4,4′-dcbpy)(tdt)] which was previously reported.[15] 5,5′-dcbpy was synthesised by oxidation of the dimethylbipyridine starting material. Reaction of 5,5′-dcbpy with potassium tetrachloroplatinate and potassium chloride gave the platinum dichloro derivative which was further reacted with toluene-3,4-dithiol to give the desired product [Pt(5,5′-dcbpy)(tdt)]. The tetrabutylammonium salt was made by reaction of a basic solution of [Pt(5,5′-dcbpy)(tdt)] with an aqueous solution of tetrabutylammonium bromide (Fig. 1).

[TBA]$_2$[Pt(5,5′-dcbpy)(tdt)] was synthesised to facilitate dissolution of the compound, since it is soluble in a range of organic solvents including methanol, ethanol, dichloro-

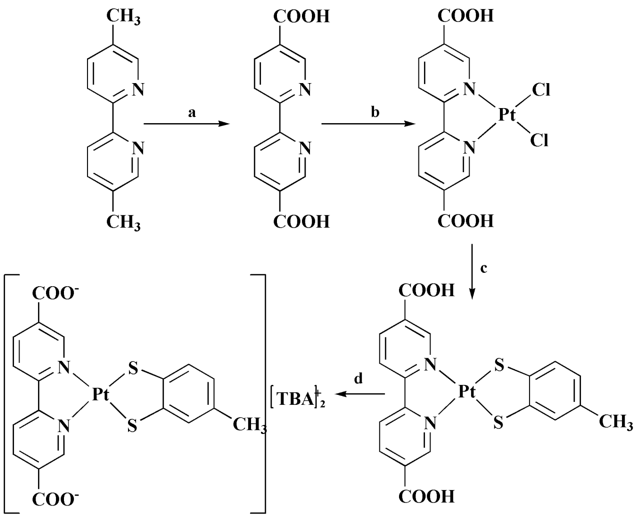

**Fig. 1** Synthesis of [Pt(5,5′-dcbpy)(tdt)] and $[TBA]_2$[Pt(5,5′-dcbpy)(tdt)]. (a) $KMnO_{4(aq)}$, 120 °C/HCl. (b) $K_2PtCl_4$, 120 °C. (c) Toluene-3,4-dithiol/KOH. (d) KOH/$TBABr_{(aq)}$.

methane, dimethylformamide and acetonitrile. The neutral [Pt(5,5′-dcbpy)(tdt)] was found to be soluble only in DMSO.

Single crystals of $[TBA]_2$[Pt(5,5′-dcbpy)(tdt)] were grown by slow diffusion of ethyl acetate into ethanol solution (Fig. 2). Only five crystal structures of Pt(diimine)(1,2-dithiolate) systems have been previously reported.[23] Four of the five feature a 4,4′-disubstituted bpy and the remaining one features an unsubstituted bpy. There are no previous reports of crystals with a 5,5′-disubstituted bpy in a Pt(diimine)(dithiolate) complex and only two other crystal structures with the 5,5′-dicarboxybpy functionality have been previously reported. Neither of these is bonded to Pt. This clearly reflects the much greater amount of study that has been carried out on 4,4′-disubstituted bpy in comparison with the 5,5′-bpy systems, presumably arising from the earlier view that the 4,4′-positions were electronically more coupled to the bpy. It may also have been influenced by the practical use of the compounds since the 5,5′-bpy systems seem to be less soluble than the 4,4′-species.[13] Bond lengths and angles are similar to those for Pt(diimine)-(dithiolate) systems previously reported.[7,24–26]

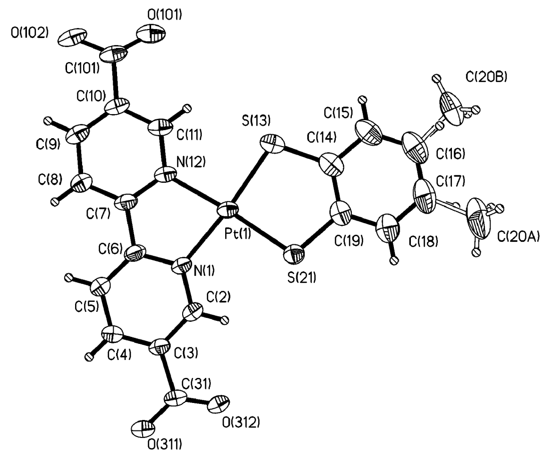

**Fig. 2** X-Ray crystal structure of $[TBA]_2$[Pt(5,5′-dcbpy)(tdt)]. Selected bond lengths (Å) and angles (°): Pt–S(13) 2.2489(7), Pt–S(21) 2.2528(7), Pt–N(1) 2.052(2), Pt–N(12) 2.047(2), C(14)–C(15) 1.393(4), C(15)–C(16) 1.374(5), C(16)–C(17) 1.393(6), C(17)–C(18) 1.379(5), C(18)–C(19) 1.391(4), C(14)–C(19) 1.396(4); N–Pt–N 79.8(8), S–Pt–S 89.48(3).

The methyl substituent on the dithiolate is disordered over two positions with a relative occupancy of 50%. The molecule is essentially planar over the whole molecule with the exception of the carboxylate groups. The bpy functionality shows a 0.0437 Å deviation from the plane and the Pt(diimine)(dithiolate) unit shows a 0.0573 Å deviation from planarity. This planarity in the molecule gives rise to the packing in layers of Pt anions separated by layers of TBA counterions. It also results in large electronic delocalisation within the molecule essential for use as a solar-cell dye.

Both [Pt(5,5′-dcbpy)(tdt)] and $[TBA]_2$[Pt(5,5′-dcbpy)(tdt)] have an intense UV band at approximately 320 nm and this band is assigned to the intraligand π–π* transition of the 5,5′-dcbpy.[27] [Pt(5,5′-dcbpy)(tdt)] shows an absorbance at 651 nm ($\varepsilon$ = 4884 $M^{-1}$ $cm^{-1}$) and $[TBA]_2$[Pt(5,5′-dcbpy)(tdt)] shows an absorbance at 558 nm ($\varepsilon$ = 3022 $M^{-1}$ $cm^{-1}$), both in DMSO (Fig. 3). These charge transfer transitions in Pt(diimine)(dithiolate) complexes have previously been assigned by Eisenberg and co-workers.[3] Charge transfer occurs from a HOMO consisting of a mixture of Pt(d) and dithiolate orbital character to a LUMO which is a low-energy π* orbital of the 5,5′-dcbpy. The absorbance maxima of the low energy band for $[TBA]_2$-[Pt(5,5′-dcbpy)(tdt)] can be tuned between 547 nm (MeCN) and 582 nm (EtOH) in a range of organic solvents, however this change in $\lambda_{max}$ values showed no obvious solvatochromic trend with respect to solvent polarity. It may be that other factors such as hydrogen bonding with the solvent also play a role in determining the energy of the band.

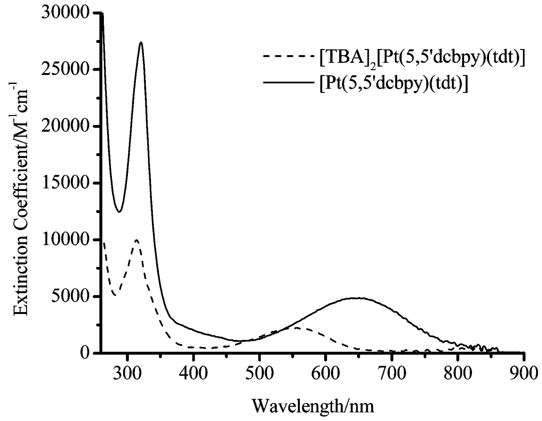

**Fig. 3** UV-vis spectra of [Pt(5,5′-dcbpy)(tdt)] and $[TBA]_2$[Pt(5,5′-dcbpy)(tdt)] in DMSO.

[Pt(5,5′-dcbpy)(tdt)] and $[TBA]_2$[Pt(5,5′-dcbpy)(tdt)] were studied by cyclic voltammetry. The cyclic voltammogram of [Pt(5,5′-dcbpy)(tdt)] in a solution of DMSO shows two reduction peaks (Fig. 4) and one oxidation peak, all of which are electrochemically reversible and showed straight line plots of $i_{max}$ *vs.* (scan rate)$^{1/2}$. The cyclic voltammogram of $[Pt(5,5'\text{-dcbpy})(tdt)]^{2-}$ in DMSO shows one reduction and three

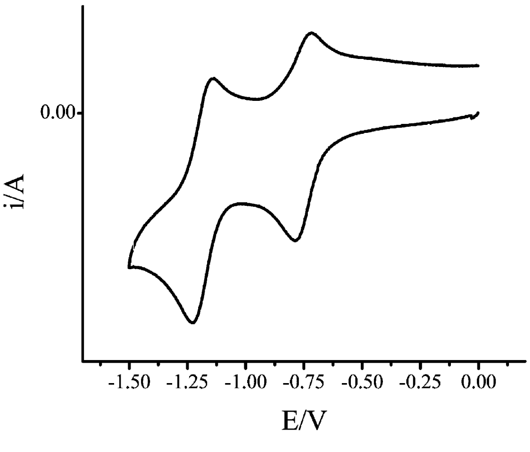

**Fig. 4** Cyclic voltammogram of [Pt(5,5′-dcpby)(tdt)] showing two bpy based electrochemically reversible reductions, scan rate 0.8 V $s^{-1}$, in 0.1 M $TBABF_4$/DMSO at 293 K.

**Table 1** Oxidation and reduction potentials for [Pt(5,5′-dcbpy)(tdt)] and $[TBA]_2$[Pt(5,5′-dcbpy)(tdt)] *vs.* Ag/AgCl

| Compound | Reduction/V | | Oxidation/V | | |
|---|---|---|---|---|---|
| [Pt(5,5′-dcbpy)(tdt)] | −1.09[a] | −0.66[a] | 0.55[a] | | |
| $[TBA]_2$[Pt(5,5′-dcbpy)(tdt)] | | −1.27[b] | 0.65[b] | 0.87[b] | 1.1[b] |

[a] Peaks are electrochemically reversible and values shown represent $E_{1/2}$. [b] Peaks are electrochemically irreversible and values shown represent peak potential.

oxidations, all of which are electrochemically irreversible. The results are shown in Table 1. Coulometric studies were performed on the oxidation of [Pt(5,5′-dcbpy)(tdt)] in an attempt to confirm the number of electrons involved in the redox process. The current passed however showed a non-integral value for electron transfer and the original complex could not be regenerated on re-reduction. This implies that during the timescale of coulometry, oxidation of [Pt(5,5′-dcbpy)(tdt)] is chemically irreversible.

It has been previously stated that the dithiolate ligand influences the oxidation potentials and the diimine ligand influences the reduction potentials of Pt(II)(diimine)(dithiolate) species, since the HOMO is partly dithiolate based and the LUMO is diimine based. The dithiolate group is identical in both [Pt(5,5′-dcbpy)(tdt)] and $[Pt(5,5'\text{-dcbpy})(tdt)]^{2-}$, hence it is expected that the oxidation potentials for both be similar. The only oxidation in [Pt(5,5′-dcbpy)(tdt)] and the first oxidation in $[Pt(5,5'\text{-dcbpy})(tdt)]^{2-}$ occur at similar potentials and this is assigned as the oxidation of the HOMO based on the dithiolate moiety in the molecule.[15] Two further oxidations are seen in $[TBA]_2$-[Pt(5,5′-dcbpy)(tdt)] at higher oxidation potentials. These oxidations may represent loss of electrons from the diimine functionality due to the carboxylate anions and lie at more positive potential. Bpy complexes generally show two reductions. Both [Pt(5,5′-dcbpy)(tdt)] and $[Pt(5,5'\text{-dcbpy})(tdt)]^{2-}$ show reduction processes, however the first reduction in $[Pt(5,5'\text{-dcbpy})(tdt)]^{2-}$ occurs at a much lower reduction potential than either of the two reductions in [Pt(5,5′-dcbpy)(tdt)], reflecting the two negative charges on the carboxylate groups of $[Pt(5,5'\text{-dcbpy})(tdt)]^{2-}$ which is more difficult to reduce than the neutral species. No second reduction can be seen for $[Pt(5,5'\text{-dcbpy})(tdt)]^{2-}$ in this solvent window.

Attempts were made to follow the redox processes occurring in both [Pt(5,5′-dcbpy)(tdt)] and $[TBA]_2$[Pt(5,5′-dcbpy)(tdt)] by spectroelectrochemistry. There were difficulties, however, with interpreting these results due to the formation of unstable redox products. Changes in the UV-Vis spectra were observed for both [Pt(5,5′-dcbpy)(tdt)] and $[Pt(5,5'\text{-dcbpy})(tdt)]^{2-}$ when the first reduction process was investigated. No isosbestic points were found for either of the compounds investigated and the original compounds could not be regenerated. The oxidation of [Pt(5,5′-dcbpy)(tdt)] was also investigated but again no isosbestic points were found and the original compound could not be regenerated. All of these results proved consistent with the coulometry results previously discussed.

We were unable to observe emission from a solution of [Pt(5,5′-dcbpy)(tdt)] in DMSO dispersed in EtOH at room temperature. In a frozen solution at 77 K emission was observed (Fig. 5). Excitation of the complex at 600 nm gives an emission spectrum with a peak at 700 nm. The corresponding excitation spectrum shows a broad band between 500 and 600 nm, consistent with the position of the absorption band of [Pt(5,5′-dcbpy)(tdt)]. Compounds of the general formula Pt(NN)(SS) are typically emissive in frozen solutions and in more recent years have been found in certain cases to emit in room-temperature solutions.[28,29] It has been stated that emission in Pt(II)(diimine)(dithiolate) species is formally a spin-forbidden process where the spin character of the emissive state is different to that of the ground state.[4] Our data appear consistent with this assignment.

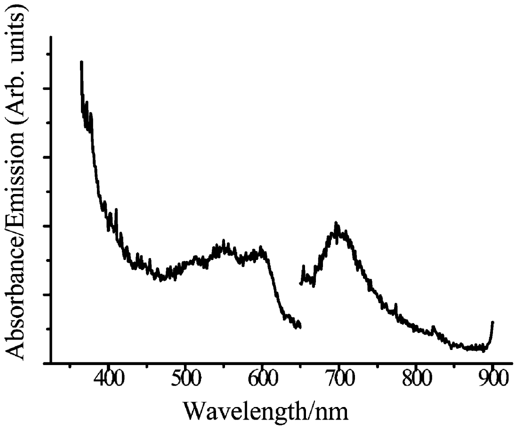

**Fig. 5** Emission and corresponding excitation spectrum of a frozen solution of [Pt(5,5′-dcbpy)(tdt)] in DMSO dispersed in EtOH.

### Evaluation of the dye as a photosensitiser

Photoelectrochemical measurements were taken in order to assess the dye as a photosensitiser. Dye binding was achieved by immersion of nanocrystalline $TiO_2$ films in a solution of the dye. Optimisation of the solvent system used for sensitisation of the films resulted in increased UV-Vis absorbance values. The optimum solution tested was a 1 : 3.2 DMSO–MeCN solution of Pt complex at a concentration of 1 mg $ml^{-1}$. These solutions were used to sensitise 8 μm $TiO_2$ films for 22 h at room temperature. The UV-Vis absorption spectrum of [Pt(5,5′-dcbpy)(tdt)] on $TiO_2$ exhibits a broad absorption band between 600 and 650 nm (Fig. 6) similar to that of the solution absorbance (651 nm) with a slight broadening and blue shift. The absorption spectrum for $[TBA]_2$[Pt(5,5′-dcbpy)(tdt)] on $TiO_2$ shows a relatively weak absorption band, red shifted (590 nm) with respect to that of the solution absorbance (558 nm). This red shift may be due to donation of electron density from the carboxylate anions to the $TiO_2$ on binding, thus making it a better electron acceptor and hence reducing the HOMO–LUMO gap. Dye loadings on

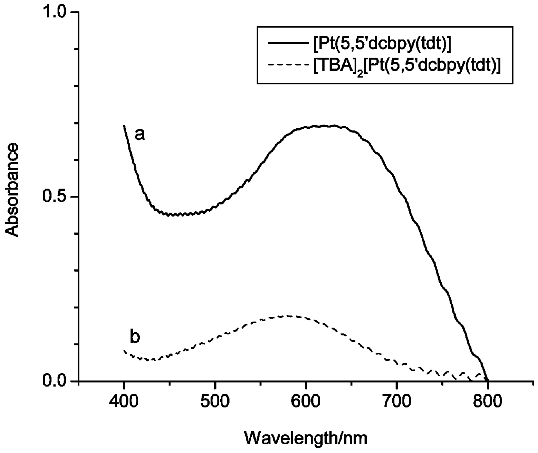

**Fig. 6** UV-vis absorption spectra of platinum dyes on $TiO_2$: (a) [Pt(5,5′-dcbpy)(tdt)], (b) $[TBA]_2$[Pt(5,5′-dcbpy)(tdt)]. Both data were collected after dipping the 8 μm $TiO_2$ film in 1 mg $ml^{-1}$ solution of the dye in DMSO ([Pt(5,5′-dcbpy)(tdt)]) and 1 : 3.2 DMSO–MeCN ($[TBA]_2$[Pt(5,5′-dcbpy)(tdt)]) for 22 h at room temperature.

**Table 2** Summary of results obtained for sensitisation of nanocrystalline $TiO_2$ films

| | Dye coverage[a]/$10^{-7}$ mol $cm^{-2}$ | Relative injection yield[b] | Recomb. half-time[c]/s | $J_{sc}$[d]/A $cm^{-2}$ | $V_{oc}$[d]/V |
|---|---|---|---|---|---|
| **1** | 1.4 | 1 | $1.7 \times 10^{-5}$ | $9.8 \times 10^{-6}$ | $8.8 \times 10^{-3}$ |
| **2** | 0.6 | 0.83 | 0.15 | $2.0 \times 10^{-5}$ | 0.19 |

[a] Dye loadings per $cm^2$ film estimated from UV-vis absorption spectra. [b] Relative yield of injected electrons per absorbed photon determined from the initial amplitude of the transient absorption signal in Fig. 7. [c] Recombination half-times determined from the transient absorption data shown in Fig. 7. [d] Current–voltage characteristics of dye sensitised photoelectrochemical cells under AM 1.5 simulated solar illumination. **1** = [Pt(5,5′-dcpby)(tdt)]. **2** = $[TBA]_2$[Pt(5,5′-dcpby)(tdt)].

the films were estimated employing the dye peak extinction coefficients determined in solution above, and are detailed in Table 2. In both cases, high dye loadings were achieved, consistent with the high surface area of the $TiO_2$ films (roughness factor ~800), with the acid form of the dye exhibiting the stronger binding.

The electron transfer function of the sensitiser dyes were evaluated by transient absorption data in the absence of redox electrolyte. Typical data are shown in Fig. 7, monitoring the photoinduced absorption of electrons injected into the $TiO_2$ following excitation of the sensitiser dyes. For both dyes, an instrument response limited rise was observed, assigned to rapid electron injection. The transient signal subsequently decays due to charge recombination between the injected electrons and the oxidised dye. The initial transient signal was largest with the [Pt(5,5′-dcbpy)(tdt)] sensitiser dye, attributed to the higher optical density obtained for the sensitised films with this dye, although in both cases the small magnitude of the transient signal was indicative of a low yield of electron injection (<10%). After normalising for differences in sample optical density, the initial signal magnitudes for the two dyes were similar, indicating similar injection yields for both dyes, as detailed in Table 2. In contrast, the charge recombination dynamics for the two sensitised films were very different, with the [Pt(5,5′-dcbpy)(tdt)] and $[TBA]_2$[Pt(5,5′-dcbpy)(tdt)] sensitised films exhibiting recombination half times of $1.7 \times 10^{-5}$ and 0.33 s, respectively. It is furthermore apparent that the shape of the transient decay are distinct for the two dyes, with the slower dynamics being less dispersive (near monoexponential), consistent with our previous observations.[30] The slower recombination dynamics for the $[TBA]_2$[Pt(5,5′-dcbpy)(tdt)] dye are indicative of weaker electronic coupling between the dye and the $TiO_2$ surface, consistent with the lower dye coverage obtained with this dye. This is presumably related to the mode of binding of the sensitiser to the $TiO_2$ surface. We do not know exactly how [Pt(5,5′-dcbpy)(tdt)] binds to $TiO_2$, however previous studies using IR spectroscopy have shown that the average mode of binding of 5,5′-dcbpy ligands in Ru complexes to $TiO_2$ to be identical to that of 4,4′-dcbpy.[13]

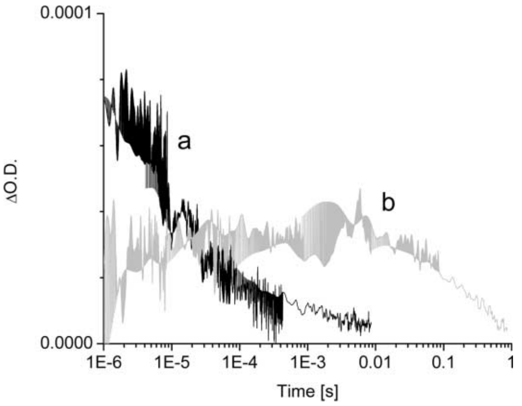

**Fig. 7** Transient absorption data monitoring the photoinduced absorption of electrons injected into the $TiO_2$ ($\lambda_{probe}$ = 1000 nm) following excitation of the sensitiser dyes at 610 nm. Data obtained for $TiO_2$ films sensitised with (a) [Pt(5,5′-dcbpy)(tdt)] and (b) $[TBA]_2$[Pt(5,5′-dcbpy)(tdt)].

Dye characterisation was further extended to characterisation of the photocurrent–voltage data for the dye sensitised $TiO_2$ in two electrode 'sandwich type' photoelectrochemical cells. Typical short circuit currents and open circuit voltages are given in Table 2. It is apparent that the better photovoltaic performance of the dyes in our study was obtained with $[TBA]_2$[Pt(5,5′-dcbpy)(tdt)], despite the lower dye loading and film optical density obtained with this dye, although for both dyes the performance is poor relative to that of [Pt(4,4′-dcbpy)(tdt)].

The electrochemistry and UV-vis spectroscopy performed on [Pt(5,5′-dcbpy)(tdt)] and $[TBA]_2$[Pt(5,5′-dcbpy)(tdt)] were consistent with related complexes[2] and allowed the analysis of the HOMO–LUMO energy gaps of the dyes. In our study, tuning the HOMO–LUMO gap was achieved by a variation made to the diimine functionality thus lowering the LUMO. In their study of Pt(diimine)(dithiolate) complexes, Arakawa and co-workers varied the dithiolate functionality of the molecule and hence altered the energy of the HOMO and the two studies show complementary results. The HOMO–LUMO energy gap as determined from the UV/Vis spectrum of both [Pt(5,5′-dcbpy)(tdt)] and $[TBA]_2$[Pt(5,5′-dcbpy)(tdt)] showed $\Delta E_{HOMO-LUMO}$ = 1.9 eV for [Pt(5,5′-dcbpy)(tdt)] and $\Delta E_{HOMO-LUMO}$ = 2.22 eV for $[TBA]_2$[Pt(5,5′-dcbpy)(tdt)]. Arakawa and co-workers showed $\Delta E_{HOMO-LUMO}$ = 2.14 eV for [Pt(4,4′dcbpy)(tdt)] in basic 4 : 1 ethanol–methanol solution. This value is comparable with our results for $[TBA]_2$[Pt(5,5′-dcbpy)(tdt)]. However, since the extent of deprotonation in [Pt(4,4′dcbpy)(tdt)] in basic 4 : 1 ethanol–methanol solution is unknown it is difficult to make a direct comparison of the HOMO–LUMO energy gaps of [Pt(4,4′-dcbpy)(tdt)] and [Pt(5,5′-dcbpy)(tdt)] from UV-Vis spectroscopic results. From the electrochemistry it can be seen that the first reduction in [Pt(5,5′-dcbpy)(tdt)] is much more facile than the first reduction in [Pt(4,4′-dcbpy)(tdt)]. This implies that placing carboxylate substituents at the 5,5′ positions of the bpy ring enhances the electron accepting ability of the complex compared to that of the 4,4′-dicarboxylate bipyridyl.

The oxidation potentials for [Pt(4,4′-dcbpy)(tdt)] and [Pt(5,5′-dcbpy)(tdt)] are comparable due to the similar nature of their dithiolate functionalities and hence their HOMOs. Thus the electrochemical data suggest we have tuned the LUMO energy to give a smaller HOMO–LUMO gap in comparison with the 4,4′-analogue. Both the present study and that of Arakawa found that dyes with longer absorption wavelengths are less efficient as solar cell sensitisers. There are a number of reasons why this may be the case.

The rate of electron injection into the conduction band of the $TiO_2$ is dependent on the height of the electronic state of the excited dye (LUMO) above the conduction band, therefore lowering the LUMO leads to less efficient electron injection to the $TiO_2$. Also, the low value of the oxidation potentials of these dyes compared to analogous dithiolate-containing complexes such as quinoxalinedithiolate (qdt) mean that regeneration of the reduced dye by the redox couple becomes more difficult due to the decrease in the energy gap between the reduced form of the redox couple ($I^-$) and the oxidised dye.[15] This results in more recombination of excited dye electrons with the oxidised dye. This is seen in both Pt species investigated here and in tdt complexes in general. Rapid charge recombination dynamics for the [Pt(5,5′-dcbpy)(tdt)] dye, is also consistent with its poorer performance relative to its di-TBA salt. Furthermore, non-radiative decay of excited electrons may also have an influence on the dye efficiency. This is governed by the energy gap law for MLCT excited states which states that the rate of non-radiative decay of a CT complex increases exponentially with the corresponding decrease in HOMO–LUMO energy gap. Complexes with the tdt moiety have consistently lower extinction coefficients when compared to other Pt(diimine)-(dithiolate) species. A lower $\varepsilon$ value means that the dye has a lower light harvesting efficiency. This is a factor in the overall IPCE (Incident-Photon-to-Current Efficiency) of the cell.

## Conclusions

This work illustrated the difficulty with long-wavelength dye molecules. There is a general difficulty with low energy absorbing dyes since in lowering the energy of the LUMO, there is a decrease in electron injection from the dye to the conduction band of the semiconductor. It may not be possible to have both the LUMO at high enough energy to overcome the driving force required for electron injection and the HOMO at low enough energy to allow efficient dye reduction by the electrolyte and still retain a long wavelength absorbance. Arakawa and co-workers experienced similar difficulties in their investigation of Pt(II)(diimine)(dithiolate) dyes. On going to longer wavelengths the performance of the dyes as photosensitisers decreased dramatically. Short-wavelength dyes with higher energy LUMOs perform better as photosensitising devices and the performance of our dye is consistent with those previously reported.

## References

1 S. D. Cummings and R. Eisenberg, *J. Am. Chem. Soc.*, 1996, **118**, 1949.

2 W. Paw, S. D. Cummings, M. A. Mansour, W. B. Connick, D. K. Geiger and R. Eisenberg, *Coord. Chem. Rev.*, 1998, **171**, 125.

3 M. Hissler, J. E. McGarrah, W. B. Connick, D. K. Geiger, S. D. Cummings and R. Eisenberg, *Coord. Chem. Rev.*, 2000, **208**, 115.

4 J. A. Zuleta, J. M. Bevilacqua, J. M. Rehm and R. Eisenberg, *Inorg. Chem.*, 1992, **31**, 1332.

5 J. A. Zuleta, J. M. Bevilacqua, D. M. Proserpio, P. D. Harvey and R. Eisenberg, *Inorg. Chem.*, 1992, **31**, 2396.

6 J. M. Bevilacqua and R. Eisenberg, *Inorg. Chem.*, 1994, **33**, 1886.

7 J. M. Bevilacqua and R. Eisenberg, *Inorg. Chem.*, 1994, **33**, 2913.

8 S. D. Cummings and R. Eisenberg, *Inorg. Chem.*, 1995, **34**, 3396.

9 M. K. Nazeeruddin, A. Kay, I. Rodicio, R. Humphry-Baker, E. Müller, P. Liksa, N. Vlachopoulos and M. Grätzel, *J. Am. Chem. Soc.*, 1993, **115**, 6382.

10 P. N. W. Baxter and J. A. Connor, *J. Organomet. Chem.*, 1988, **355**, 193.

11 L. Jack, PhD Thesis, University of Edinburgh, 2003.

12 E. J. L. McInnes, R. D. Farley, S. A. Macgregor, K. J. Taylor, L. J. Yellowlees and C. C. Rowlands, *J. Chem. Soc., Faraday Trans.*, 1998, **94**, 2985.

13 R. Argazzi, C. A. Bignozzi, T. A. Heimer, F. N. Castellano and G. J. Meyer, *Inorg. Chem.*, 1994, **33**, 5741.

14 A. Islam, H. Sugihara, K. Hara, L. P. Singh, R. Katoh, M. Yanagida, Y. Takahashi, S. Murata and H. Arakawa, *New J. Chem.*, 2000, **24**, 343.

15 A. Islam, H. Sugihara, K. Hara, L. P. Singh, R. Katoh, M. Yanagida, Y. Takahashi, S. Murata, H. Arakawa and G. Fujihashi, *Inorg. Chem.*, 2001, **40**, 5371.

16 F. H. Case, *J. Am. Chem. Soc.*, 1946, **68**, 2574.

17 G. M. Sheldrick, SADABS University of Göttingen, Germany, 2002.

18 G. M. Sheldrick, SHELXTL, University of Göttingen, Germany, 1997.

19 P. v. d. Sluis and A. L. Spek, *Acta Crystallogr., Sect. A*, 1990, **46**, 194.

20 S. A. McGregor, E. J. L. McInnes, R. J. Sorbie and L. J. Yellowlees, in: *Molecular Electrochemistry of Inorganic, Bioinorganic and Organometallic Compounds*, ed. A. J. L. Pombeiro and J. A. McCleverty, Kluwer, Dordrecht, 1993, p. 503.

21 R. L. Willis, C. Olson, B. O'Regan, T. Lutz, J. Nelson and J. R. Durrant, *J. Phys. Chem. B*, 2002, **106**, 7605.

22 E. Palomares, J. Clifford, S. Haque, T. Lutz and J. Durrant, *J. Am. Chem. Soc.*, 2003, **125**, 475.

23 Cambridge Structural Database F. H. Allen and O. Kennard, *Chem. Des. Autom. News*, 1993, **8**, 31.

24 C. E. Keefer, R. D. Bereman, S. T. Purrington, B. W. Knight and P. D. Boyle, *Inorg. Chem.*, 1999, **38**, 2294.

25 C. J. Adams, *J. Chem Soc., Dalton Trans.*, 2002, 1545.

26 W. B. Connick and H. B. Gray, *J. Am. Chem. Soc.*, 1997, **119**, 11620.

27 S. D. Cummings and R. Eisenberg, *Inorg. Chem.*, 1995, **34**, 2007.

28 D. L. Webb and L. A. Rossiello, *Inorg. Chem.*, 1971, **10**, 2213.

29 F. Barigelletti, D. Sandrini, M. Maestri, V. Balzani, A. Von Zelewsky, L. Chassot, P. Joillet and U. Maeder, *Inorg. Chem.*, 1988, **27**, 3644.

30 J. N. Clifford, G. Yahioglu, L. R. Milgrom and J. R. Durrant, *Chem. Commun.*, 2002, 1260.